Stress-strain model of lower corroded steel plates of normal strength for fitness-for-purpose analyses

Krzysztof Woloszyk[a], Yordan Garbatov[b, 1], Paweł Kłosowski[c]

[a] Institute of Naval Architecture and Ocean Engineering, Gdansk University of Technology, G. Narutowicza 11/12 st., 80-233 Gdansk, Poland

[b] Centre for Marine Technology and Ocean Engineering (CENTEC), Instituto Superior Técnico, Universidade de Lisboa, Avenida Rovisco Pais 1049-001 Lisboa, Portugal

[c] Faculty of Civil and Environmental Engineering, Gdansk University of Technology, G. Narutowicza 11/12 st., 80-233 Gdansk, Poland

Abstract

This study investigates the mechanical properties of specimens made of normal strength steel subjected to lower marine immersed corrosion degradation levels (below 25 %). The specimens were corroded in laboratory conditions, and only natural factors were controlled to raise the corrosion rate (reaching the level of 1 mm/year). Three different thicknesses of plates made of normal strength of shipbuilding steel are investigated (between 5 mm and 8 mm). The standard tensile tests are performed for estimating the stress-strain behaviour of corroded specimens. Non-corroded specimens were tested to establish the initial mechanical properties and uncertainty level as a reference. Further, the corroded specimens were tested too. Based on that, the changes in mechanical properties (i.e. yield stress, Young modulus, ultimate tensile stress and total elongation) were analysed. It was found, that for degradation level reaching 25%, approx. 10% reduction of yield stress was observed. A new parameter, defining the area reduction, was established as more closely related to the mechanical properties deterioration than the commonly used a mean degradation level. The bilinear stress-strain model of corroded steel plates was proposed for the fitness-for-purpose analyses in the structural integrity assessment.

Keywords: corrosion, mechanical properties, marine environment, fitness-for-purpose

[1] Corresponding author e-mail: yordan.garbatov@tecnico.ulisboa.pt; Telf (351) 21 841 7907

1 Introduction

Ships and offshore structures operating at sea are subjected to a highly corrosive environment. The non-uniform corrosion degradation is a factor that can significantly affect the load-carrying capacity of different structural members [1–4], mainly due to cross-sectional area reduction and decrease of mechanical properties. One can identify the most common types of corrosion, like pitting and general corrosion [5]. The examples of these two corrosion types that could be found in ship structures are distinguished in industrial guidelines, such as [6], where examples of real corroded structures are presented (see Figure 1). Pitting corrosion is a very localised degradation phenomena that results in the creation of small holes in the metal. On the other hand, general corrosion is spread within the entire surface, but degradation level is non-uniform within the structural components. These two types of corrosion need to be treated separately in terms of modelling and analysis.

Figure 1. The comparison between general (left) and pitting corrosion (right) [6].

The corrosion causes not only general thickness loss but also a reduction of mechanical properties. This, in consequence, could result in a collapse of various structural components or even entire structure. Thus, the investigation of this phenomenon is of crucial importance from the safety point of view. Recently, more studies related to that problem were performed. When dealing with ship structures, most important are flat specimens, taken from thin-walled structural elements. One of the first attempts to investigate the mechanical properties of corroded steel specimens with different corrosion severity were made by Garbatov et al. [7]. In this case, the typical coupon specimens were taken from a corroded box girder [8], which was corroded in seawater with the additional electric current applied. The corrosion degradation level of specimens was very high in that case and varied between 25% up to 75%. It was found that all mechanical properties were reduced, i.e. yield strength, Young’s modulus, ultimate tensile stress and total elongation. The observed reduction of yield stress was around 15% for degradation level of 50%, and mean thickness after corrosion was taken as the reference to calculate the mechanical properties.

The mechanical properties of corroded flat-bar specimens subjected to atmospheric corrosion were investigated too. Samples taken from truss corroded in natural atmospheric conditions with different thicknesses were tested in [9], showing significant mechanical properties reduction. In this case, the corrosion degradation level varied between 17% and 34%. For 25% of degradation level, the observed reduction of yield stress was around 14%. However, in this case, the maximum residual thickness was considered as the reference value for the calculation of mechanical properties.

Very thin specimens of 1 mm subjected to atmospheric corrosion were tested in [10], and the observed reduction of mechanical properties reached the level of 70%, for the degradation level of 40%. Also in this case, maximum residual thickness after corrosion was taken as the reference value. Atmospherically corroded specimens with lower values of corrosion degradation were tested in [11], showing that above 15% of degradation level, there is an evident decrease of mechanical properties. Some other works related to the mechanical properties of steel elements subjected to atmospheric corrosion may be found in [12–15].

The tensile testing of corroded specimens was also performed regarding circular bars. The stress-strain behaviour of corroded circular bars was investigated by Kashani et al. [16], and the degradation level was up to 20%. The concrete elements with bars were corroded in salt water with the application of electric current. The observed reduction of yield strength was up to 30%, and the total elongation was reduced up to 80%. In the study of Zhan et al. [17], the 267 naturally and artificially corroded specimens have been tested, showing the significant deterioration of mechanical properties and shortening or even disappearing yield plateau. Other works related to the mechanical properties of corroded bars may be found in [18–22], leading to similar conclusions.

Based on the listed works, the reduction of mechanical properties of flat-bar specimens as well as bars with the corrosion development was evident. Further, it could be concluded that the reduction of mechanical properties has been observed for both severely degreded specimens and lower corrosion degradation levels related to the steel structures in operation. However, it can be noted that the reduction of mechanical properties is different for different studies. Thus, more experimental work is needed to establish more general relationships accounting for type of corrosion considered. In addition, different reduction levels were obtained for flat-bar specimens and for bars.

It was also found, that the reduction of mechanical properties is mainly caused by the local non-uniformities of the surfaces of the corroded specimens [23–26]. For ideally uniformly corroded specimens, the reduction of mechanical properties will be not visible, supported by the experimental results presented in [27]. The specimens after cleaning showed higher mechanical properties than the corroded non-cleaned ones. Additionally, when the FE analysis was performed, taking into account only non-uniformities in corroded surfaces [28,29], the results were similar to those obtained experimentally.

In the marine environment and especially for ship structures, general corrosion with local non-uniformities is the most common, and this phenomenon cannot be neglected, and in this respect, mathematical models showing the loss of mechanical properties as a function of corrosion development need to be developed. Some models based on the limited experimental data exist for corroded bars [30–32]. In case of flat-bar specimens, most of studies deals with atmospheric corrosion [9–13]. Only the study performed by Garbatov et al. [7] could be noticed in the case of marine immersed corrosion. However, in this case and most of other studies, the corrosion was accelerated by the application of electric current. It has been shown in [33] that when specimens are corroded with the DC power input source application, the corrosion morphology will be different from those obtained in natural conditions. Higher non-uniformity in thickness distribution is observed for naturally corroded specimens.

The presented work extends analyses of the mechanical properties of steel specimens subjected to immersed marine corrosion degradation for a lower corroded level of steel specimens. The previous research was mainly devoted to the specimens subjected to atmospheric corrosion, whereas studies related to marine immersed corrosion are lacking. The limited works related to marine immersed corrosion were focused on rather higher levels of degradation. Furtherly, the corrosion was fastened by the application of electric current. In the present study, the specimens were corroded in laboratory conditions by the acceleration of only natural factors. The detailed information regarding corrosion tests could be found in [34]. Nevertheless, the main features are briefly outlined in the text. Three different groups of thicknesses and different corrosion degradation levels were examined. Based on the tensile test results, the changes in mechanical properties depending on the lower corrosion degradation level were analysed. The bilinear stress-strain model of lower corroded steel plates is proposed for the fitness-for-purpose analyses in the structural integrity assessment.

2 Experimental set-up and corrosion testing

The three different thicknesses of plates made of normal shipbuilding strength steel of S235 (which is also used in other branches of technology under different symbols) were the objective of the current study, namely 5 mm, 6 mm and 8 mm thicknesses. Although corrosion resistant steels are available, due to their high price, the typical constructional steel is commonly used. The chemical composition of steel, as provided by the manufacturer, is presented in Table 1. Although the plates were made from one batch of the steel, the hot-rolling process caused a slight difference in the chemical composition of plates with different thicknesses. Standard coupon specimens (fabricated according to the ISO norm

[35]) from each thickness of standard size (see Figure 2) were taken from different places of steel sheets (1.25 m x 2.5 m) and analysed. In each thickness, six or seven specimens were used to obtain the mechanical properties in an intact state, whereas ten samples were subjected to the accelerated marine immersed corrosion degradation. In case of intact plates, a such number of specimens provided a minimum reliable database regarding the mean values of mechanical properties and their scatter. In case of corroded specimens, such number leads to an examination of changes in mechanical properties with the corrosion development with the low difference between subsequent degradation levels.

Table 1. Chemical composition of tested steel specimens.

Thickness [mm]	**Fe [%]**	**C [%]**	**Si [%]**	**Mn [%]**	**S [%]**	**P [%]**	**Cu [%]**	**Al [%]**	**N [%]**
5	99.2	0.1	0.01	0.48	0.013	0.025	0.04	0.03	0.004
6	99.1	0.12	0.03	0.51	0.011	0.015	0.06	0.03	0.004
8	99.0	0.13	0.024	0.67	0.012	0.023	0.026	0.03	0.004

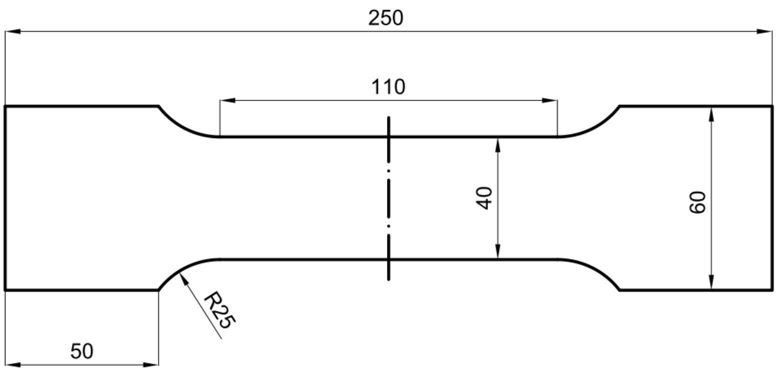

Figure 2. Dimensions of standard coupon specimens [mm].

The corrosion test set-up has been already presented in [36], and the results of corrosion tests have been widely discussed in [34]. Thus, only main information regarding corrosion testing is provided.

The coupon specimens were corroded in a 900-litre tank made from glass reinforced plastic laminate, together with larger-sized stiffened plates. The corrosion testing set-up is presented in Figure 3, showing the small-scale specimens placed on the supporting structure. The corrosion rate was increased by the aeration pump (2) (oxygen content increase), heaters (3) (temperature increase) and circulation pumps (4). The salinity level was set equal to 35 ppm by mixing freshwater with natural sea salt. The governing parameters were initially assumed: 35°C, 300% oxygen content concerning supersaturation conditions, and a water speed of 0.03 m/s. The corrosion rate estimated initially was equal to 0.736 mm/year [36]. The corrosion testing tends to provide a specific level of degradation within initially assumed time frames, where the governing factors were constant. Corrosion testing could also possibly account for natural temperature or water velocity fluctuations. This could be done by setting the temperature controller and circulation pumps controller for specific function that will change the factors within time. However, in present study, factors were assumed to be constant. The total duration of the corrosion test was 428 days. Additional circulation pumps have been applied to increase the water velocity due to the lower oxygen level than initially assumed (around 200%). The mean corrosion rates were 0.649 mm/year, 1.009 mm/year and 1.025 mm/year for 5 mm, 6 mm and 8 mm specimens, respectively [34].

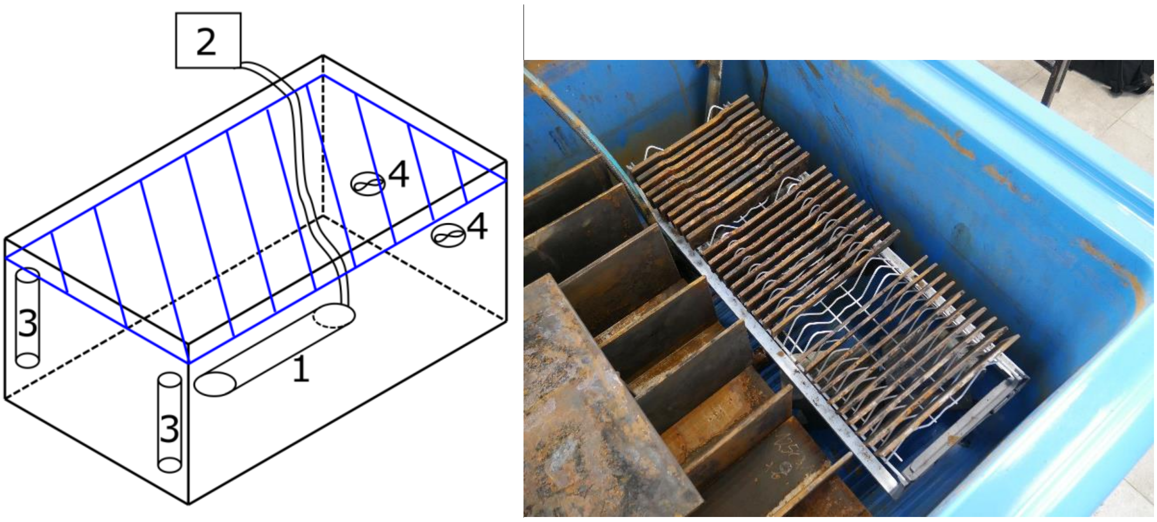

Figure 3. Corrosion test set-up [34] (1- linear diffuser, 2 – aeration pump, 3 - heaters, 4 – circulation pumps) (left) and corrosion tank with placed specimens (right).

The target levels of corrosion degradation, that were aimed to achieve during the design of set-up were: 3%, 6%, 8%, 10%, 12%, 14%, 16%, 18%, 20%, 21%, which respect the operational level of corroded steel plates before they are replaced at 25% degradation in structures in operation. Due to an increasing level of uncertainty in the severe corrosion degradation, the intervals of the degradation level were smaller for severely corroded specimens. The final corrosion degradation levels, obtained from mass measurements, are presented in Table 2. Additionally, the corrosion surface's statistical descriptors are obtained based on the information gathered from the scanning of the specimens, as described in [34], including maximum and minimum thickness, minimum cross-sectional area and standard deviations of corrosion diminutions. Notably, a significant level of surface non-uniformity was observed (see Figure 4, bottom).

Both surfaces of the specimens were scanned separately. In some cases, the standard deviation of the corrosion depth measured in one side of the specimen reached the level of 0.84 mm. Before measurements, the specimens were cleaned. The scanning provided information about the surface non-uniformities (only one surface could be scanned at a time), whereas degradation level was obtained based on mass measurements. The example of the corroded specimen after cleaning, during scanning, is presented in Figure 4.

Figure 4. Example of the specimen during scanning (top) and example of reproduced surface (bottom).

It needs to be highlighted that actual degradation levels were slightly different from those assumed initially. There were two reasons for that. Firstly, the specimens were cleaned after corrosion degradation. The actual mass was somewhat lower than that measured directly after testing. Secondly, for strength evaluation, only corrosion characteristics of specimens without mounting parts are relevant. Thus, based on the scanning results, the degradation level of the gauge part was determined.

In most cases, the differences were not exceeding 2 % of degree-of-degradation (DoD), concerning the degradation level for the whole specimen. The DoD level is considered as the percentage of the initial mass of the specimen due to corrosion degradation. Thus, it is the mean level of corrosion degradation of each specimen. The DoD will depend on the time of corrosion degradation, which could be noticed in [34]. However, for strength testing, the DoD level is the most important. The final degradation levels for each thickness are presented in Table 2. The mechanical properties were determined according to mean thickness after corrosion degradation, i.e. accounting for degradation levels shown in Table 2. Determining mechanical properties concerning the mean value of thickness is practical since it can be obtained by ultrasonic measurements periodically performed in ships and offshore structures. Based on the mean thickness reduction, the *DoD* and changes in mechanical properties may be estimated. Further, as DoD increase, the level of surface non-uniformity also increase. Thus, DoD accounts for non-uniformity in corroded surfaces implicitly, but is more practical to be determined in operating structure.

Table 2. Degradation levels of specimens, considering gauge section only.

Thickness [mm]	**Degradation level in ascending order for subsequent specimens [%]**									
	No. 1	No. 2	No. 3	No. 4	No. 5	No. 6	No. 7	No. 8	No. 9	No. 10
5	3.2	5.9	7.4	8.0	13.1	15.4	15.4	15.5	16	24.3
6	2.2	6.3	6.8	9.6	12.3	14.1	14.7	16.6	17.6	21.3
8	1.7	4	12.3	13.8	14.1	14.8	15.6	16.9	18.4	28.4

The standard Zwick-Roell Z400 machine with a step electric engine was used to conduct the tensile test and estimate the elasticity modulus, where a mechanical extensometer was adopted (see Figure 5). The tests were performed following the ISO standard for tensile testing [35] of flat coupons, and the loading was displacement-driven. The strain rate was 0.00025 mm/mm/s up to the moment, where the yield point has been reached. Above the yield point, the strain rate was 0.002 mm/mm/s. The distance between heads was 170 mm.

Figure 5. Testing machine (left) and mounted specimen with installed extensometer (right).

3 Stress-strain behaviour of intact specimens

Six to seven intact specimens of each thickness were tested before corrosion degradation to identify the initial mechanical properties. The obtained engineering stress-strain curves are presented in Figure 6.

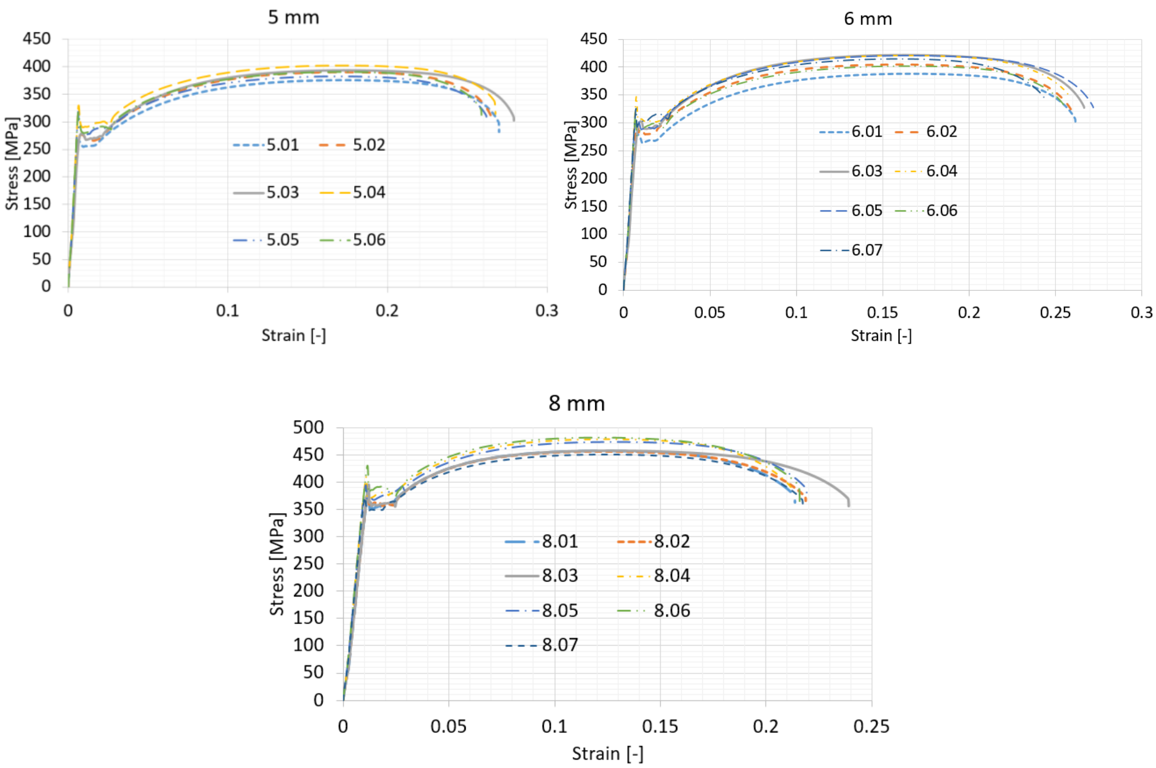

Figure 6. Stress-strain curves for 5 mm, 6 mm and 8 mm intact specimens.

The summary of performed tensile tests is presented in Table 3. In the case of elastic modulus, very similar results in different thicknesses were obtained. However, for both yield stress and ultimate tensile stress, the values are different for each thickness. The yield stress has been considered the lower yield point. The elastic modulus was calculated as the mean inclination of the stress-strain curve in the region between 20 % and 80 % of the yield stress. Notably, the yield stress value is higher than the normative value of 235 MPa for that steel grade. The 5 mm and 6 mm specimens presented similar total elongation, whereas 8 mm specimens were of the lower ductility. It could also be noted that some features typical for the material type rather than thickness are similar, i.e. evident yield plateau and stress-strain relationship after the beginning of yielding. Further, the mechanical properties are subjected to a significant level of uncertainty. The highest uncertainty is observed for a 5 mm plate in the yield stress, and the Coefficient of Variation is 4.5 %. In general, the level of uncertainty oscillates between 3 % and 4.5 % of CoV for different properties.

Table 3. Tensile tests for intact specimens.

Thickness [mm]	**Parameter**	**Young's modulus E [GPa]**	**Yield stress R_e [MPa]**	**Ultimate tensile stress R_m [MPa]**	**Total elongation δ [-]**
5	Mean	197.42	272.25	389.19	0.266
	Standard Deviation	10.43	12.31	9.15	0.01
	Coefficient of Variation [-]	0.053	0.045	0.024	0.027
6	Mean	196.38	284.36	410.30	0.260
	Standard Deviation	7.57	12.57	12.66	0.01
	Coefficient of Variation [-]	0.039	0.044	0.031	0.034
8	Mean	199.08	360.61	465.15	0.219
	Standard Deviation	6.84	11.83	12.55	0.01
	Coefficient of Variation [-]	0.034	0.033	0.027	0.041

4 Stress-strain behaviour of corroded specimens

After cleaning and measuring the corroded specimens, there were subjected to tensile testing. As a result, the stress-strain relationship for each specimen has been obtained, and all testing parameters have been registered. The stresses were calculated regarding the mean thickness value, estimated based on the degradation level, as reported in Table 2.

The stress-strain relationships for 5 mm specimens for different DoD were presented in Figure 7. Additionally, the reference stress-strain curve, for $DoD = 0\%$ was added, which was taken from tests of intact specimens. The curve that resulted in the highest value of yield stress from several specimens was considered in this case. This graph shows evident degradation of mechanical properties, including the yield stress, ultimate tensile stress, and total elongation. Further, the yield plateau is smaller with corrosion development and even disappearing for severely corroded specimens than intact specimens (see Figure 6).

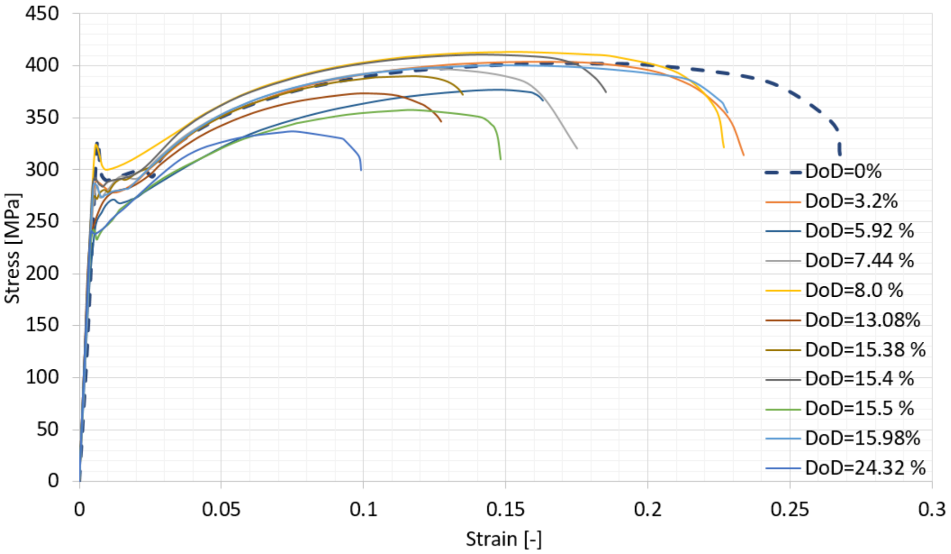

Figure 7. Stress-strain relationships for 5 mm specimens subjected to corrosion degradation

Similar observations could be captured for other groups of thicknesses. The stress-strain relationships for 6 mm specimens are presented in Figure 8, whereas for the 8 mm specimens are shown in Figure 9. The most evident differences in changes in the yield stress could be noticed in Figure 9 for the 8 mm specimens. In the 6 mm specimens, those changes are smaller (see also Table 4). Nevertheless, a lack of the yield plateau for severely corroded specimens and a significant drop of total elongation is purely visible in both cases.

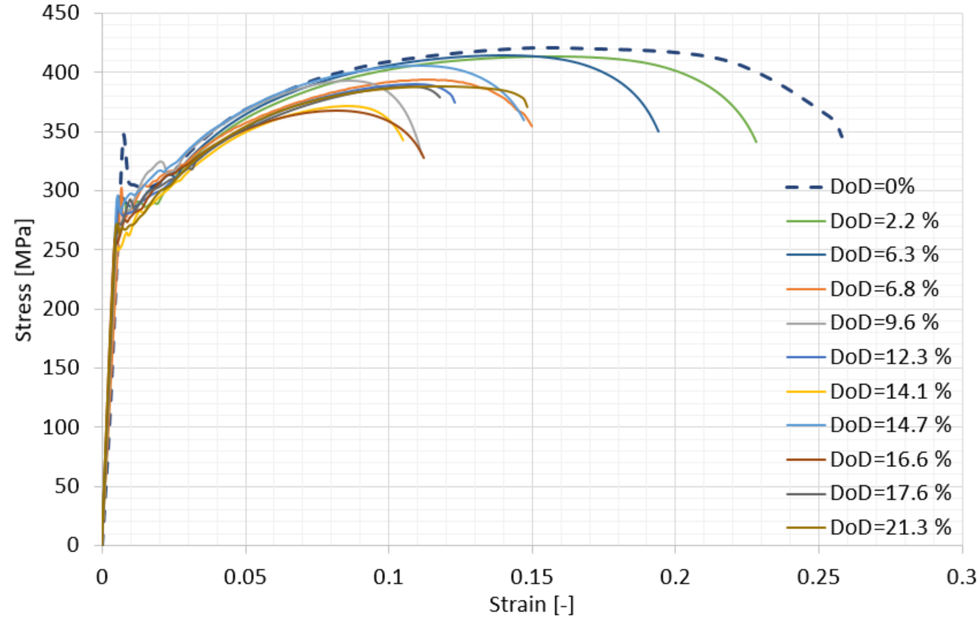

Figure 8. Stress-strain relationships for 6 mm specimens subjected to corrosion degradation

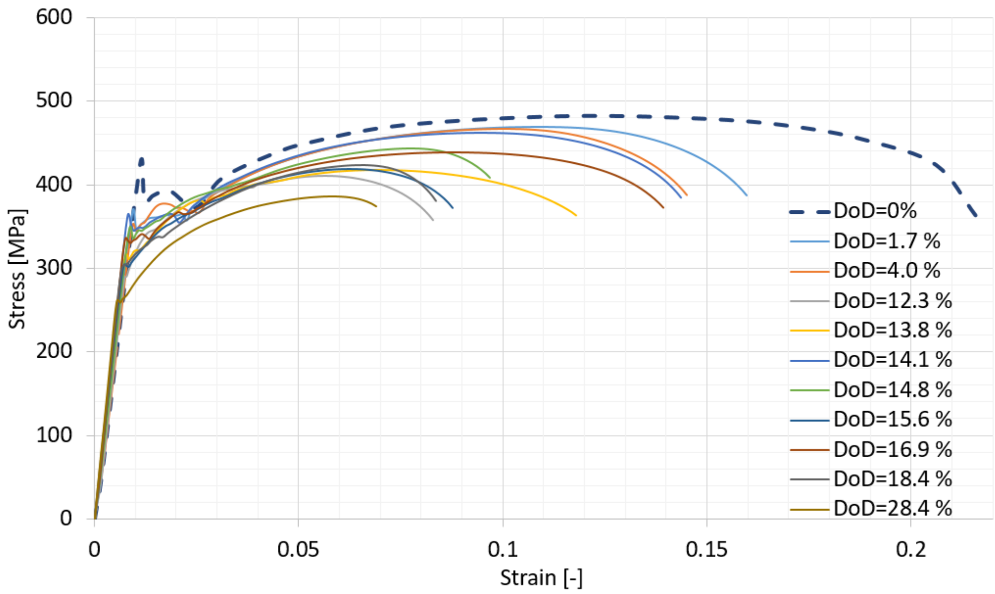

Figure 9. Stress-strain relationships for 8 mm specimens subjected to corrosion degradation

The detailed results are presented in Table 4. From the beginning, a large scatter of mechanical properties is observed. There are two sources of this phenomenon. Firstly, significant scatter was observed for the intact specimens of mechanical properties (see Table 3). Secondly, since the corrosion process introduces a stochastic origin, the mechanical properties are dependent on those, resulting in additional scatter. Thus, to observe the relation between DoD and mechanical properties, there were grouped by similar degradation levels, i.e., group 1 (between 0 % and 8 % of DoD), group 2 (between 8 % and 16 % of DoD) and group 3 (above 16 % of DoD). Additionally, one point from 5 mm thickness was excluded from further analysis due to the very high yield stress and ultimate tensile stress values, exceeding the maximum values observed for intact specimens (see Figure 7). The division of specimens into groups is presented in Table 4 regarding each thickness.

Table 4. Detailed results of mechanical properties for corroded specimens.

Thickness [mm]	DoD [%]	E [Gpa]	R_e [Mpa]	R_m [Mpa]	Elongation [-]	Group
5	3.2	234.8	278.1	404.0	0.234	1
	5.9	208.0	253.2	377.0	0.163	
	7.4	219.9	273.1	397.5	0.175	
	8.0	202.1	300.0	413.3	0.227	excluded
	13.1	238.0	247.9	373.6	0.127	2
	15.4	236.9	271.7	389.8	0.134	
	15.4	256.6	283.6	410.3	0.185	
	15.5	221.1	232.7	356.9	0.148	
	16.0	235.5	273.8	400.0	0.228	3
	24.3	187.1	238.0	336.6	0.099	
6	2.2	192.9	281.3	413.5	0.229	1
	6.3	200.8	286.1	414.5	0.195	
	6.8	203.0	273.5	393.4	0.150	
	9.6	211.9	270.0	392.8	0.112	2
	12.3	242.1	278.3	390.1	0.123	
	14.1	202.4	249.7	371.5	0.106	
	14.7	247.4	281.0	405.3	0.151	
	16.6	214.7	255.1	367.9	0.113	3

	17.6	258.6	271.3	387.7	0.119	
	21.3	208.5	264.3	388.6	0.148	
8	1.7	221	343.8	469.5	0.161	1
	4.0	234.1	344.5	467	0.146	
	12.3	226.3	307	410.8	0.083	2
	13.8	215.6	310.2	417.2	0.118	
	14.1	220.6	344.8	462.1	0.144	
	14.8	226.1	335.3	443.1	0.098	
	15.6	187.5	299.9	418.6	0.088	
	16.9	219	334.5	438.4	0.14	3
	18.4	222.7	303.2	423.2	0.084	
	28.4	204.5	258.4	385.8	0.069	

To investigate the changes in mechanical properties with the progress of corrosion degradation, the results for each thickness are plotted as a function of the Degree of Degradation. For each group, the mean value of both DoD and respective mechanical properties is calculated. Thus, the points in graphs are not representing the values for particular specimens but mean values for different groups of degradation levels (groups 1, 2 and 3), as presented in Table 4. Additionally, the error bars showing the standard deviation of each group are presented. The corrosion dependent mechanical properties for 5 mm specimens were presented in Figure 10. The mechanical properties for DoD = 0 % are considered as the mean value from tensile tests performed for intact specimens and there are reported in Table 3 for each thickness separately.

Further, the regressions are found, considering that for $DoD = 0\%$, the values are known and equal to initial values. As outlined in the last part of the text, the results of Young's modulus were inaccurate and thus, no regressions were established. This methodology is adopted similarly for other thicknesses.

The evident reduction of mechanical properties is observed. In the case of yield stress and ultimate tensile stress, the linear regressions are plotted. There were found to have the highest correlation for different thicknesses. For total elongation, the exponential regression was found to represent its changes with corrosion development. Although a similar correlation factor is found for the linear regression, this will result in negative values of that parameter for higher values of DoD. In the case of exponential regression, the value will always be positive and tend to be near-zero value for $DoD = 100\ \%$. The observed correlation factors for the yield stress is very high, whereas lower values were obtained for ultimate tensile stress and total elongation.

However, there was found no correlation between Young's modulus and degradation level. Very high elastic modulus values were obtained for some mean corrosion depths, significantly exceeding its value for intact specimens, even considering uncertainty level (see Figure 10). Thus, such values obtained experimentally should be considered false. The same observation is obtained for other thicknesses, i.e. 6 mm (Figure 11) and 8 mm (Figure 12).

There are several possible reasons for such a situation. In the case of the yield stress, ultimate stress and total elongation, these characteristics somehow represent the entire specimen's behaviour. However, in Young's modulus, the strain is measured via an extensometer between two points near the specimen's middle. In the prismatic specimen, this is purely valid, whereas, in the case of a corroded specimen, this does not show the entire specimen's behaviour. As reported by corrosion scans, there are cases with areas of a higher thickness in the middle of the specimen, which will lead to relatively low strains when the mean thickness is considered a reference. Notably, the places of failure of the specimens were, in most cases, away from the middle (see Figure 13). Thus, the obtained Young's modulus for the corroded specimens cannot be considered. The elastic modulus could be considered a constant for the whole DoD range and equal to the one obtained for intact specimens.

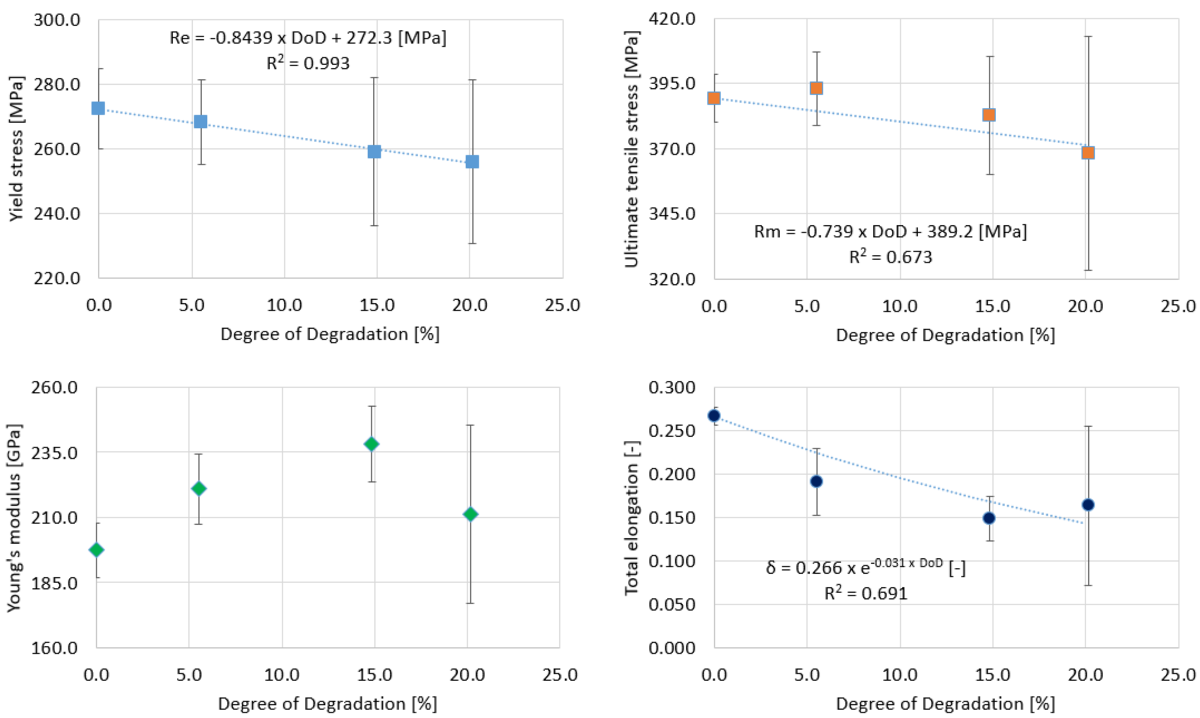

Figure 10. Mechanical properties as a function of DoD, 5 mm specimens.

The changes in mechanical properties for 6 mm specimens are presented in Figure 11. It is noted that there was observed a similar reduction of the yield stress, whereas ultimate tensile stress degraded faster in comparison to 5 mm specimens. It is noted that very high correlation factors were obtained for each mechanical property (except for elastic modulus).

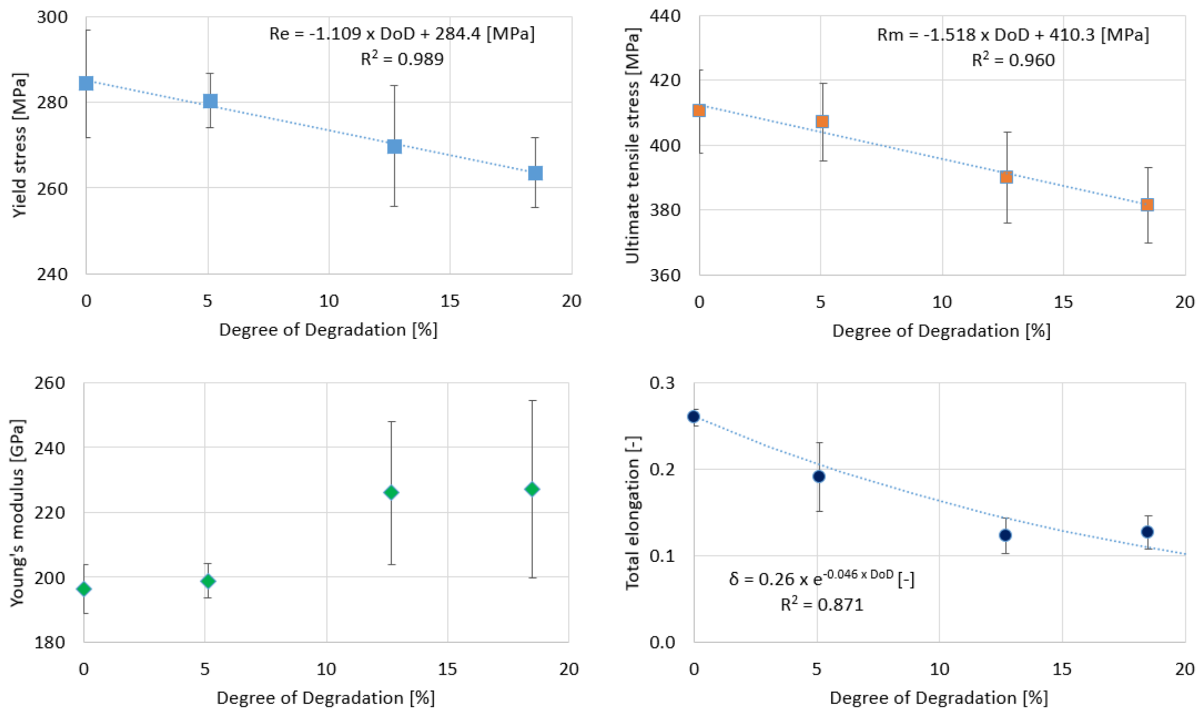

Figure 11. Mechanical properties as a function of DoD, 6 mm specimens.

The corrosion-dependent mechanical properties for the 8 mm specimens are presented in Figure 12. Notably, the observed reduction of mechanical properties is significantly higher than other thicknesses, regardless of the higher initial values of the yield stress and ultimate tensile stress (see Table 3). Similarly to 6 mm specimens, very high correlation factors has been observed.

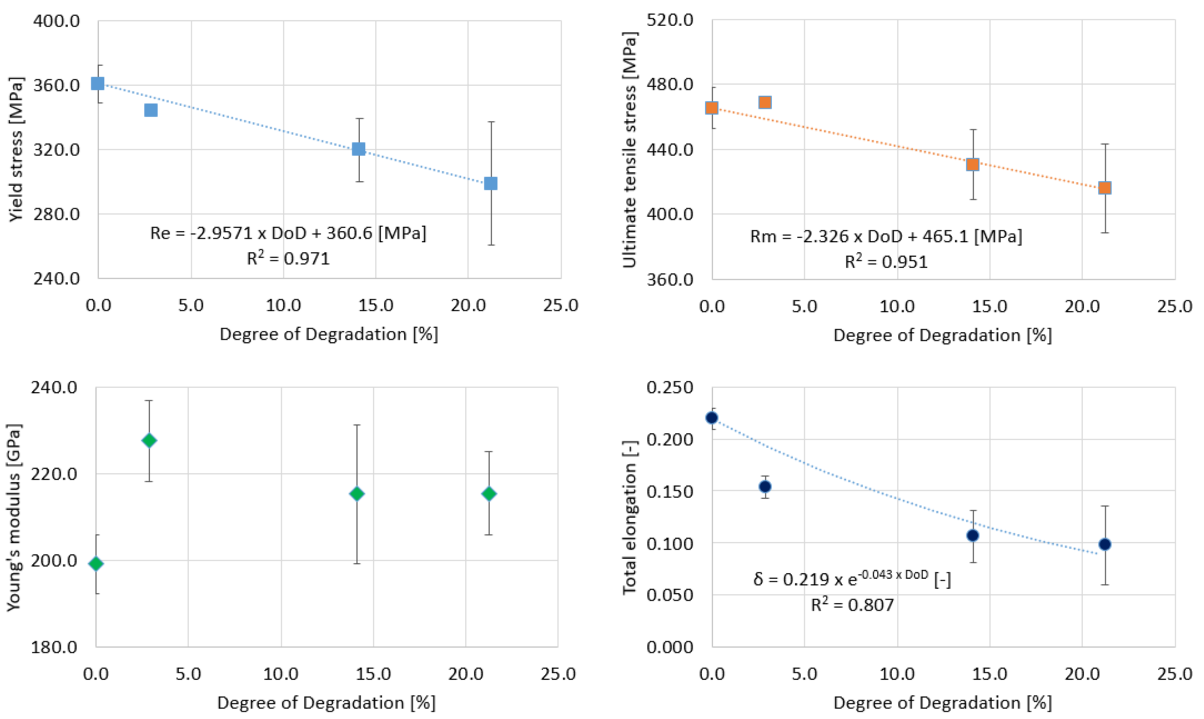

Figure 12. Mechanical properties as a function of DoD, 8 mm specimens.

It could also be noted that lower correlation coefficient values have been observed in the case of 5 mm plates (Figure 10). It could be concluded that the lower correlation for 5 mm plates was caused by relatively high uncertainty of both material properties and corrosion characteristics. Notably, for 8 mm plates, a higher decrease of material properties has been observed, which dominated the observed scatter of the results.

By comparing the presented results with other available data, it is noted, that with comparison to marine immersed corrosion accelerated with the application of electric current [7], higher reduction of yield stress was observed. In the case of the present study, for $DoD = 25\%$, the yield stress was reduced by approximately 10%. In the case of [7], a 15% reduction was noted for $DoD = 50\%$. When compared with naturally atmospherically corroded specimens [9], the observed reduction for $DoD = 25\%$ was similar to the present study. However, the maximum residual thickness was considered as the reference to calculate the mechanical properties.

Figure 13 shows examples of failure modes of tested specimens. It could be noticed that the failure mode is different in comparison to typically observed for intact specimens. In most cases, the cross-section, where the breaking line is followed, is related to the position, where the minimum cross-sectional area along the gauging part is located [29]. Further, the breaking line is non-straight and inclined in most cases, which is not the case of intact specimens, where a straight line is usually noted perpendicular to the loading direction.

Figure 13. The examples of tested specimens with a thickness of 5 mm (top), 6 mm (mid) and 8 mm (bot).

Different studies noted that the yield stress's degradation level is most probably related to the minimum cross-sectional area obtained along with the specimen. Therefore, to verify that, the normalised yield stress (yield stress of corroded specimen divided by the mean yield stress of intact specimen) is compared with the normalised reduction factor of minimal cross-sectional area. In this case, the results for single specimens are investigated since the area reduction is related to any particular specimen. However, since the material properties are estimated based on the cross-sectional area, which is associated with the mean value thickness of the corroded specimen, the normalised reduction factor of cross-sectional area is proposed as follows:

$$AR = \frac{A_0\left(1-\frac{DoD}{100}\right)-A_{min}}{A_0\left(1-\frac{DoD}{100}\right)}\ [-] \tag{1}$$

where A_0 is the initial cross-section area of non-corroded specimen and A_{min} is the minimum cross-sectional area.

The proposed factor informs how much the minimum cross-sectional area is smaller concerning the mean cross-sectional area. In other words, factor shows the percentage difference between minimum cross-sectional area and cross-sectional area, if corrosion will cause the uniform reduction of thickness. The bigger the AR factor is, the smaller the cross-sectional area is as a percentage of the mean cross-sectional area of the corroded specimen. Figure 14 (left) shows the results from different thicknesses collated and the relation between the yield stress and reduction factor. A similar statistical analysis, as in the case of Figures 10 to 12 was adopted herein. Thus, the experimental points were grouped within similar AR factors levels, and each group's standard deviation is presented in the graph.

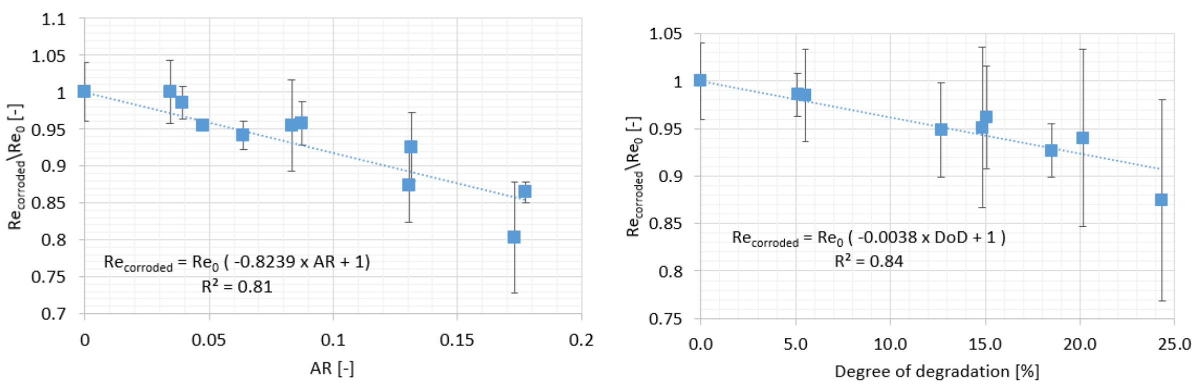

Figure 14. Relation between normalised yield stress and cross-sectional area reduction factor (left) and between normalised yield stress and DoD (right).

It is noted that a good correlation between these two parameters is observed. Except for several points, the observed scatter is in the order of yield stress uncertainty. Although a similar correlation between the reduction factor and yield stress was achieved compared to DoD and yield stress (see

Figure 14 - right), the scatter for particular groups is significantly smaller. The linear correlation was the most suitable for both cases presented in Figure 14, resulting in the highest correlation coefficient. This indicates that not always the degradation level is the most appropriate parameter that informs about the state of a corroded structure. A similar correlation was found between area reduction factor and normalised ultimate tensile strength and normalised total elongation, respectively (see Figure 15). In the case of ultimate tensile strength, the linear correlation resulted in the highest correlation factor, whereas, the exponential regression was most appropriate for a total elongation. Similarly to the yield stress, the area reduction factor is more related to the corrosion-dependent material properties than the Degree of Degradation level. The correlations between DoD and normalised ultimate tensile stress and total elongation were 0.59 and 0.71, respectively (see Figure 16). Similarly to yield stress, the single data points are significantly less scattered with comparison to the regressions based on DoD (see Figure 16).

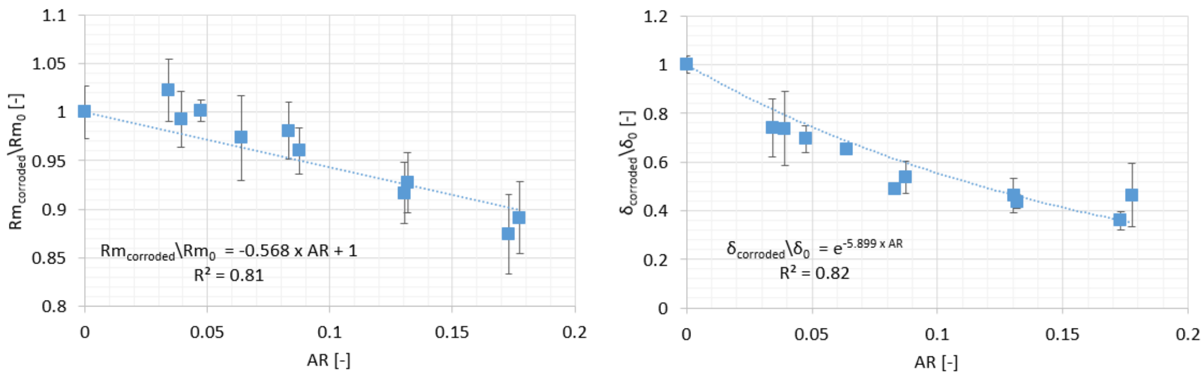

Figure 15. Relation between cross-sectional area reduction factor and normalised ultimate tensile strength (left) and normalised total elongation (right).

Although AR factor seems to be more suitable to predict the degradation of material properties, its determination requires very detailed surface recognition. Thus, for engineering applications, DoD is more convenient, estimated based on simple thickness measurements. Additionally, by grouping the results, the compensation of uncertainty related to area reduction may be obtained.

Based on the presented results, one could draw the hypothesis that the thicker plate is, the higher reduction of mechanical properties is observed. However, it will be somewhat premature to make conclusions, and more investigations will be needed at this staged. Especially, there were no significant differences in reduction levels in the case of 5 mm and 6 mm specimens, and only 8 mm specimens presented a higher level of mechanical properties decrease. It could result from slightly different corrosion characteristics obtained for a diverse group of thicknesses. It was found that the area reduction factor was the main reason for the deterioration of material properties. This factor was slightly higher for the 8 mm specimens than others, and thus, the material properties were also lower.

5 Stress-strain model for fitness-for-purpose analyses

Since the mechanical properties themselves are subjected to relatively high scatter, it is reasonable to consider changes in mechanical properties obtained from various initial thicknesses. This will increase the total number of experimental points and derive some constitutive laws regardless of the specimen's initial thickness, which could be helpful to fitness-for-purpose analyses.

Since different initial mechanical properties were obtained for different thicknesses, the relative values of mechanical properties with the corrosion degradation progress are estimated. Thus, for a particular DoD, the observed value of the parameter is divided by its value in a non-corroded state. Young's modulus is assumed to be constant within the whole DoD range.

Figure 16 presents the collected results obtained from the tested specimens (considering results for groups), and the regression relationships have been derived, leading to general constitutive laws. Similarly to previous relationships (Figures 10-12), the linear regression led to the highest regression coefficients for yield and ultimate tensile stresses. In the case of total elongation, both linear regression and exponential one resulted in a similar regression coefficient. However, the exponential was chosen to avoid negative values of the total elongation for higher values of the degradation level, similarly as in Figures 10-12.

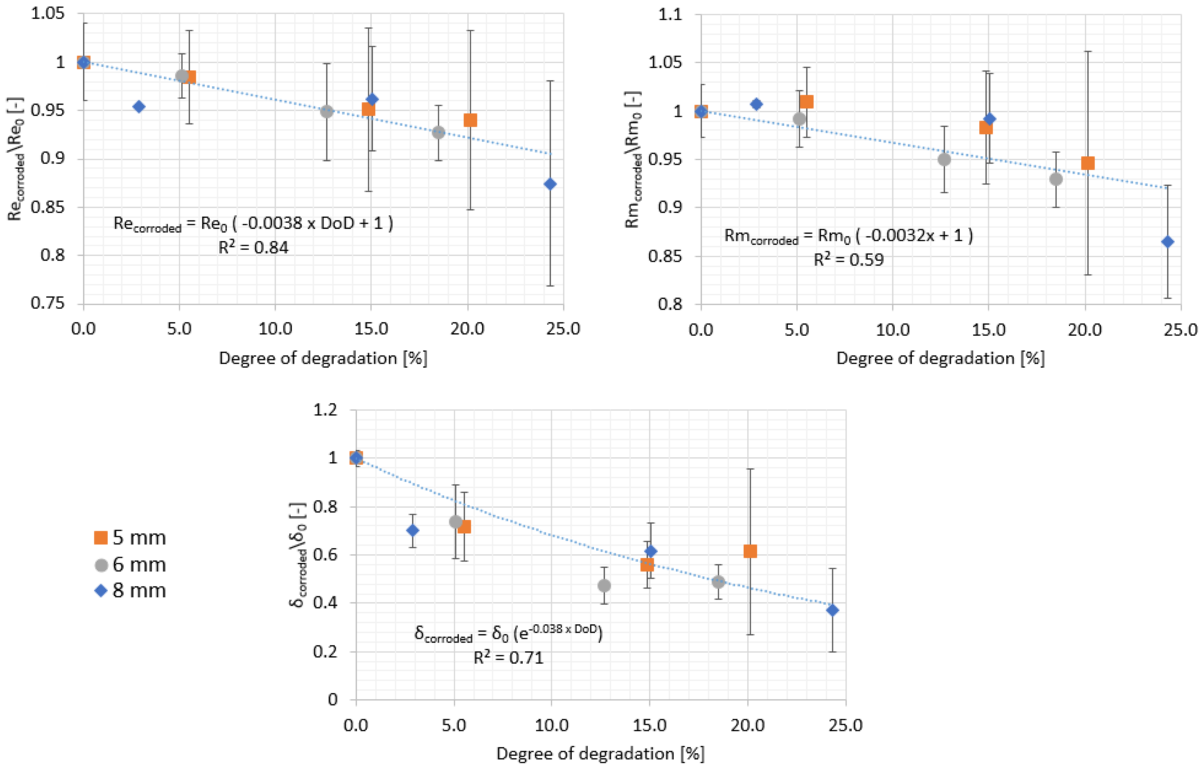

Figure 16. Normalised mechanical properties in function of DoD.

The standard deviation is calculated since any particular point is scattered from the assumed regression relationship. The variation for a specific point is calculated as a difference between the experimental and predicted values by the regression model. In Young's modulus, the standard deviation is calculated based on the tests carried out for the intact specimens (see Table 3).

The standard deviation results are as follows (Young's modulus – Eq. 2, Yield stress – Eq. 3, Ultimate tensile stress – Eq. 4, Total elongation – Eq. 5):

$$E_{StDev} = 0.0402\ E_0[GPa] \tag{2}$$

$$Re_{StDev} = 0.0556\ Re_0\ [MPa] \tag{3}$$

$$Rm_{StDev} = 0.0431\ Rm_0\ [MPa] \tag{4}$$

$$\delta_{StDev} = 0.145\ \delta_0\ [-] \tag{5}$$

The presented parameters could be used for the reliability analysis of ship structural components subjected to corrosion degradation, e.g. [37,38].

Further, for a different type of FE analysis, usually, the bilinear stress-strain model is used. It needs to be noted that a true stress-strain relationship should be used instead of an engineering one. According to [39], the true stress-strain relationship from the start of yielding up to the moment where the maximum load is reached could be determined via the following equation:

$$\sigma = K\varepsilon^n \tag{6}$$

where n is the strain hardening exponent, K is the strength coefficient and ε_p is the plastic strain.

To identify the parameters K and n, the log-log plot of the relationship from Eq. 6 could be established, leading to the linear relationship and fitted to the experimental data from all specimens. The stress-strain relationship in the logarithmic scale will be the linear relationship followed by the equation $y = ax + b$, where a is equal to n and b is the logarithm of K.

Further, to identify the failure strain in a bilinear model, the modulus of toughness could be useful, given by the equation:

$$U_t = \int_0^{\varepsilon_f} \sigma d\varepsilon \tag{7}$$

which represents the energy that is needed to break the specimen.

The values of K, n and U_t were identified for each specimen. However, since different initial material properties were observed for different thicknesses, the normalised parameters were introduced, except the strain hardening parameter. The strength coefficient is divided by the initial yield stress of considered thickness, and the modulus of toughness is divided by the multiplication of yield stress and total elongation value. The relationships between degradation level and normalised parameters are presented in Figure 17.

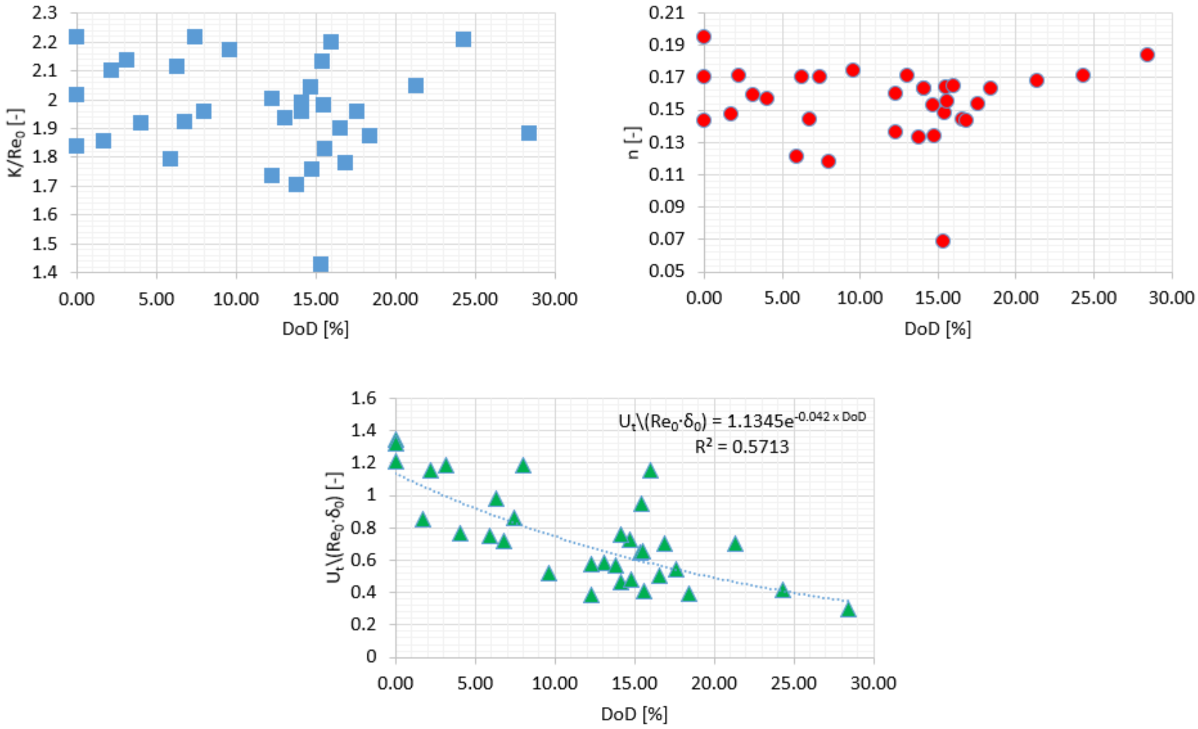

Figure 17. Relationships between normalised parameters of stress-strain relationships and degradation level.

The regression analysis was performed and different functions were studied for all variables. For the normalised strength the R^2 value is not exceeding 0.02, and in the case of the strain hardening parameter, the regression coefficient was 0.2 for the polynomial regression. It could be concluded that there is no correlation between these variables and DoD. Thus, the mean values of $K/Re_0 = 1.958$ and $n = 0.154$ are considered. In the case of modulus of toughness, the non-linear regressions were found to result in highest R^2 values – namely, the polynomial and exponential ones. However, the polynomial function presented a local minimum for DoD equal to 30%, and the modulus of toughness will increase after crossing that value. This will be non-concise with the physical representation of the phenomena. Thus, the exponential equation has been found for the normalised modulus of toughness, as given in Figure 17.

Based on the information provided in both Figures 16 and 17, the bilinear stress-strain relationships dependent on corrosion level are defined as follows (considering DoD up to 25 %):

$$\sigma = \begin{cases} E\varepsilon & (\varepsilon < \varepsilon_1) \\ \sigma_1 = Re_0(1 - 0.0061 \cdot DoD) & \left(\varepsilon = \varepsilon_1 = \dfrac{\sigma_1}{E}\right) \\ \sigma_1 + \dfrac{(\varepsilon - \varepsilon_1)(\sigma_2 - \sigma_1)}{\varepsilon_2 - \varepsilon_1} & (\varepsilon_1 < \varepsilon < \varepsilon_2) \\ \sigma_2 = \sigma_1 + 1.958 \cdot Re_0 \cdot \varepsilon_2^{0.154} & (\varepsilon = \varepsilon_2) \end{cases} \tag{8}$$

where ε_2 is defined in that the area under the bilinear stress-strain relationship is equal to the modulus of toughness for the particular degradation level.

Conclusions

The presented study investigated the mechanical properties of corroded steel subjected to immersed marine corrosion degradation. It was found that even for a lower degradation level (below 25%), with comparison to previously conducted studies (e.g. [7]), the mechanical properties of mild steel could have significantly deteriorated. This is highly important since such levels of degradation are typically allowed in the operating ship and offshore structures. By comparing the presented results with other available data, it was found that marine immersed corrosion brings the higher decrease of mechanical properties. Notably, not only strength characteristics were deteriorated, but deformability (i.e. total elongation) was significantly reduced (even below 15%). This could cause problems in crashworthiness of structures, e.g. in ship collision problems.

The presented results were subjected to significant scatter caused by the variability in mechanical properties of intact specimens (due to inconsistencies in chemistries, processing temperatures, cooling patterns, the strip thickness and numerous other factors [40]) and corrosion degradation. Thus, the specimens of similar degradation levels were grouped for the analysis. In addition, the non-uniformity of the corroded surfaces caused problems in the estimation of the elastic modulus. Particularly, the typical mechanical extensometer that measures the elongation between two points was found to be impractical. More advanced techniques, e.g. optical extensometer or Digital Image Correlation equipment, seems to be needed for future studies to investigate the relationship between stress distribution within specimen and degradation level. Further, the microstructure of corroded specimens could be studied via X-ray micro tomography and adopted in FE model of corroded specimens. This will allow to understand the relation between stresses and microstructure of corroded specimens.

It was found that although degradation level is easy to be measured in operating structure, it is not that related to changes of mechanical properties with comparison to other parameters. Specifically, the normalised area reduction factor, related to minimum cross-sectional area, was more correlated with the drop of mechanical properties due to corrosion. However, this will require detail surface recognition of corroded elements, with the use, e.g. 3-D scanning techniques or photogrammetry measurements. This will require high working effort. Thus, future studies should look for other governing parameters, particularly easily measured in a real structure or better diagnostic techniques allowing to gather more information regarding corroded elements in less amount of time.

As the primary outcome of a presented analysis, the bilinear stress-strain relationships of corroded steel were proposed together with uncertainty factors regarding the values of mechanical properties. Such relationships can be used for fitness-for-purpose analyses in the structural integrity assessment of corroded structures (including ships, offshore structures and onshore harbour facilities). For example, this could be adopted in FE analysis of corroded structural elements, where degradation level will be estimated based on the thickness measurements, and material will be modelled based on the proposed relationships. However, in present study, thickness range between 5 mm up to 8 mm study was investigated. The relationships for other thicknesses need to be studied in future, since higher thicknesses are often used in marine structures.

Acknowledgements

This research was funded by The National Science Centre, Poland (grant No. 2018/31/N/ST8/02380, entitled “Experimental and numerical investigations of progressive collapse of ageing structures exposed to corrosion and locked cracks”).

References

[1] Melchers RE. Development of new applied models for steel corrosion in marine applications including shipping. Ships Offshore Struct 2008;3:135–44.

[2] Guedes Soares C, Garbatov Y, Zayed A, Wang G. Corrosion wastage model for ship crude oil tanks. Corros Sci 2008;50:3095–106.

[3] Bai Y, Jin W-L. Reassessment of Jacket Structure. Mar. Struct. Des., Elsevier; 2016, p. 875–89.

[4] Woloszyk K, Kahsin M, Garbatov Y. Numerical assessment of ultimate strength of severe corroded stiffened plates. Eng Struct 2018;168:346–54.

[5] Wang Y, Wharton JA, Shenoi RA. Ultimate strength analysis of aged steel-plated structures exposed to marine corrosion damage: A review. Corros Sci 2014;86:42–60.

[6] International Association of Classification Societies. Recommendation 87. Guidelines for coating maintanance & repairs for ballast tanks and combined cargo/ballast tanks on oil tankers. 2015.

[7] Garbatov Y, Guedes Soares C, Parunov J, Kodvanj J. Tensile strength assessment of corroded

small scale specimens. Corros Sci 2014;85:296–303.

[8] P. Domzalicki, I. Skalski, C. Guedes Soares YG. Large Scale Corrosion Tests. In: P.K. Das, editor. Anal. Des. Mar. Struct., Taylor & Francis Group; 2009, p. 193–8.

[9] Wang Y, Xu S, Wang H, Li A. Predicting the residual strength and deformability of corroded steel plate based on the corrosion morphology. Constr Build Mater 2017;152:777–93.

[10] Nie B, Xu S, Yu J, Zhang H. Experimental investigation of mechanical properties of corroded cold-formed steels. J Constr Steel Res 2019;162:105706.

[11] Qin G, Xu S, Yao D, Zhang Z. Study on the degradation of mechanical properties of corroded steel plates based on surface topography. J Constr Steel Res 2016;125:205–17.

[12] Xu S, Zhang H, Wang Y. Estimation of the properties of corroded steel plates exposed to salt-spray atmosphere. Corros Eng Sci Technol 2019;54:431–43.

[13] Xu S, Zhang Z, Li R, Wang H. Effect of cleaned corrosion surface topography on mechanical properties of cold-formed thin-walled steel. Constr Build Mater 2019;222:1–14.

[14] Wu H, Lei H, Chen YF. Grey relational analysis of static tensile properties of structural steel subjected to urban industrial atmospheric corrosion and accelerated corrosion. Constr Build Mater 2021:125706.

[15] Jia C, Shao Y, Guo L, Liu Y. Mechanical properties of corroded high strength low alloy steel plate. J Constr Steel Res 2020;172:106160.

[16] Kashani MM, Crewe AJ, Alexander NA. Nonlinear stress-strain behaviour of corrosion-damaged reinforcing bars including inelastic buckling. Eng Struct 2013;48:417–29.

[17] Zhang W, Shang D, Gu X. Stress-strain relationship of corroded steel bars. Tongji Daxue Xuebao/Journal Tongji Univ 2006;34.

[18] Fernandez I, Berrocal CG. Mechanical Properties of 30 Year-Old Naturally Corroded Steel Reinforcing Bars. Int J Concr Struct Mater 2019;13:9.

[19] Li L, Mahmoodian M, Li CQ. Effect of corrosion on mechanical properties of steel bridge elements. 9th Int. Conf. Bridg. MAINTENANCE, Saf. Manag., 2018.

[20] Li L, Li C-Q, Mahmoodian M. Effect of Applied Stress on Corrosion and Mechanical Properties of Mild Steel. J Mater Civ Eng 2019;31:04018375.

[21] Ren C, Wang H, Huang Y, Yu Q-Q. Post-fire mechanical properties of corroded grade D36

marine steel. Constr Build Mater 2020;263:120120.

[22] Franceschini L, Vecchi F, Tondolo F, Belletti B, Sánchez Montero J. Mechanical behaviour of corroded strands under chloride attack: A new constitutive law. Constr Build Mater 2022;316:125872.

[23] Du YG, Clark LA, Chan AHC. Residual capacity of corroded reinforcing bars. Mag Concr Res 2005;57:135–47.

[24] Cairns J, Plizzari GA, Du Y, Law DW, Franzoni C. Mechanical properties of corrosion-damaged reinforcement. ACI Mater J 2005;102:256–64.

[25] Du YG, Clark LA, Chan AHC. Effect of corrosion on ductility of reinforcing bars. Mag Concr Res 2005;57:407–19.

[26] Palsson R, Mirza MS. Mechanical response of corroded steel reinforcement of abandoned concrete bridge. ACI Struct J 2002;99:157–62.

[27] Garbatov Y, Saad-Eldeen S, Guedes Soares C, Parunov J, Kodvanj J. Tensile test analysis of corroded cleaned aged steel specimens. Corros Eng Sci Technol 2018:1–9.

[28] Woloszyk K, Garbatov Y. Random field modelling of mechanical behaviour of corroded thin steel plate specimens. Eng Struct 2020;212:110544.

[29] Woloszyk K, Garbatov Y. An enhanced method in predicting tensile behaviour of corroded thick steel plate specimens by using random field approach. Ocean Eng 2020;213:107803.

[30] Moreno E, Cobo A, Palomo G, González MN. Mathematical models to predict the mechanical behavior of reinforcements depending on their degree of corrosion and the diameter of the rebars. Constr Build Mater 2014;61:156–63.

[31] Fernandez I, Bairán JM, Marí AR. Mechanical model to evaluate steel reinforcement corrosion effects on σ-ε and fatigue curves. Experimental calibration and validation. Eng Struct 2016;118:320–33.

[32] Li D, Xiong C, Huang T, Wei R, Han N, Xing F. A simplified constitutive model for corroded steel bars. Constr Build Mater 2018;186:11–9.

[33] Xiao L, Peng J, Zhang J, Ma Y, Cai CS. Comparative assessment of mechanical properties of HPS between electrochemical corrosion and spray corrosion. Constr Build Mater 2020;237:117735.

[34] Woloszyk K, Garbatov Y, Kowalski J. Indoor accelerated controlled corrosion degradation test of small- and large-scale specimens. Ocean Eng 2021;241:110039.

[35] ISO. Metallic materials - Tensile testing - Part 1: Method of test at room temperature. Int Stand ISO 6892-1 2009.

[36] Woloszyk K, Garbatov Y. Accelerated large scale test set-up design in natural corrosion marine environment. In: Guedes Soares C, Santos TA, editors. Dev. Marit. Technol. Eng., London: CRC Press; 2021, p. 517–24.

[37] Woloszyk K, Garbatov Y. Reliability of corroded stiffened plate subjected to uniaxial compressive loading. Int J Marit Eng 2020;162 (A4):421–30.

[38] Woloszyk K, Garbatov Y. Structural Reliability Assessment of Corroded Tanker Ship Based on Experimentally Estimated Ultimate Strength. Polish Marit Res 2019;26:47–54.

[39] Kwesi Nutor R. Using the Hollomon Model to Predict Strain-Hardening in Metals. Am J Mater Synth Process 2017;2:1–4.

[40] Bright GW, Kennedy JI, Robinson F, Evans M, Whittaker MT, Sullivan J, et al. Variability in the mechanical properties and processing conditions of a High Strength Low Alloy steel. Procedia Eng 2011;10:106–11.